GEOPHYSICAL RESEARCH LETTERS, VOL. 28, NO. 6, PAGES 1147-1150, MARCH 15, 2001

First medium energy neutral atom (MENA) images of Earth's magnetosphere during substorm and storm-time

C.J. Pollock,[1] K. Asamura,[2] M.M. Balkey,[3] J.L. Burch,[1] H.O. Funsten,[4] M. Grande, [5] M. Gruntman,[6] M. Henderson,[4] J.-M. Jahn,[1] M. Lampton,[7] M.W. Liemohn,[8] D.J. McComas,[1] T. Mukai,[2] S. Ritzau, [4] M.L. Schattenburg,[9] E. Scime,[3] R. Skoug,[4] P. Valek[1,10] and M. Wüest[1]

Abstract. Initial ENA images obtained with the MENA imager on the IMAGE observatory show that ENAs emanating from Earth's magnetosphere at least crudely track both *Dst* and *Kp*. Images obtained during the storm of August 12, 2000, clearly show strong ring current asymmetry during storm main phase and early recovery phase, and a high degree of symmetry during the late recovery phase. Thus, these images establish the existence of both partial and complete ring currents during the same storm. Further, they suggest that ring current loss through the day side magnetopause dominates other loss processes during storm main phase and early recovery phase.

1. Introduction

Energetic ions in Earth's magnetosphere charge exchange with the extended neutral atmosphere to produce energetic neutral atoms (ENA) that are imaged by ENA 'cameras' on the Imager for Magnetopause-to-Aurora Global Exploration (IMAGE) observatory [*Burch et al.*, 2000.] The Low (LENA; [*Moore et al.*, 2000), medium (MENA; [*Pollock et al.*, 2000]) and high (HENA; [*Mitchell et al.*, 2000]) energy neutral atom imagers on IMAGE observe ENAs from 15 eV up to 500 keV per nucleon, allowing visualization of the magnetosphere. This enables exploration of global structures and processes, and their response to solar wind driving.

The ring current, plasma sheet, cusp, and their low altitude extensions produce ENA fluxes in the MENA energy range. Increases in ENA flux are induced by plasma injections associated with geomagnetic storms and substorms [*Roelof,* 1987; *Henderson et al.,* 1997], as well as by enhanced magnetospheric convection [*Liemohn et al.,* 1999; *M. Thomsen,* private communication, 2000]. At IMAGE, the dominant source of ENAs above a few keV is the ring current. ENA fluxes are therefore expected to correlate with ring current enhancements as indexed by *Dst* [*Tinsley,* 1979; *Williams et al.,* 1992; *Fok et al.,* 1996; *Jorgensen et al.,* 1997]. Ring current ENAs have been discussed from the point of view of mid-latitude aurora and plasma heating by *Prölss* [1973] and, with photometric observations, by *Tinsley* [1979]. Tinsley cited *Dessler and Parker* [1959] and *Sckopke* [1966] in noting the proportionality of the time derivative $d(Dst)/dt$ and ring current loss processes, including ENA emissions. *Roelof et al.* [1985] discussed ring current loss by ENA emission and the implication of the Dessler-Parker-Sckopke relation in detail. Using the CEPPAD instrument on Polar, *Jorgensen et al.* [1997] found that storm time 30–50 keV ENA flux was proportional to *Dst*, particularly during storm recovery.

Observations consistent with an incomplete or asymmetric ring current have been presented and discussed e.g. by *Frank et al.* [1970], *Kawasaki and Akasofu* [1971], and *Greenspan and Hamilton* [2000]. Recently, models [*Liemohn et al.* 1999] have shown a compact asymmetric ring current during storm main phase, and its evolution into a larger, more symmetric configuration during late recovery. This is due to enhanced convection during the main phase, which places the bulk of the ring current on open drift paths. Decreasing convection during recovery allows the ring current to grow radially and become more symmetric as drift paths circumscribe the Earth.

We present initial MENA observations and compare them with both *Dst* and *Kp*, thereby demonstrating the sensitivity of observed ENA rates at IMAGE to magnetospheric activity. From the morphology of the ENA fluxes observed during the storm of August 12, 2000, we clearly observe evolution from a compact, asymmetric ring current during main phase to an expanded and more symmetric one during late recovery.

2. Observations

MENA images respond sensitively to geomagnetic activity and graphically portray magnetospheric dynamics. We present observations from two days. One (July 26, 2000) displayed mildly disturbed ($Kp = 3 - 4$) conditions. The other (August 12, 2000) allows study of storm dynamics and global ring current evolution.

July 26, 2000 Figure 1 shows a full day of observations from July 26, 2000. This day was mildly active, with two instances of enhanced activity (Figure 1f). Most of the day was characterized by negative IMF B_z component (mean value at ACE between 0400 and 2300 UT was -6.1 nT). Solar wind speed and density displayed typical values near 350 km s^{-1} and 10 cm^{-3}.

[1]Southwest Research Institute, San Antonio, TX
[2]Institute of Space and Astronautical Sciences, Japan
[3]West Virginia University, Morgantown, WV
[4]Los Alamos National Laboratory, Los Alamos, NM
[5]Rutherford Appleton Laboratory, Oxfordshire, England
[6]University of Southern California, Los Angeles, CA
[7]University of California at Berkeley, Berkeley, CA
[8]University of Michigan, Ann Arbor, MI
[9]MIT Center for Space Research, Cambridge, MA
[10]Auburn University, Auburn, AL

Paper number 2000GL012641.
0094-8276/01/2000GL012641$05.00

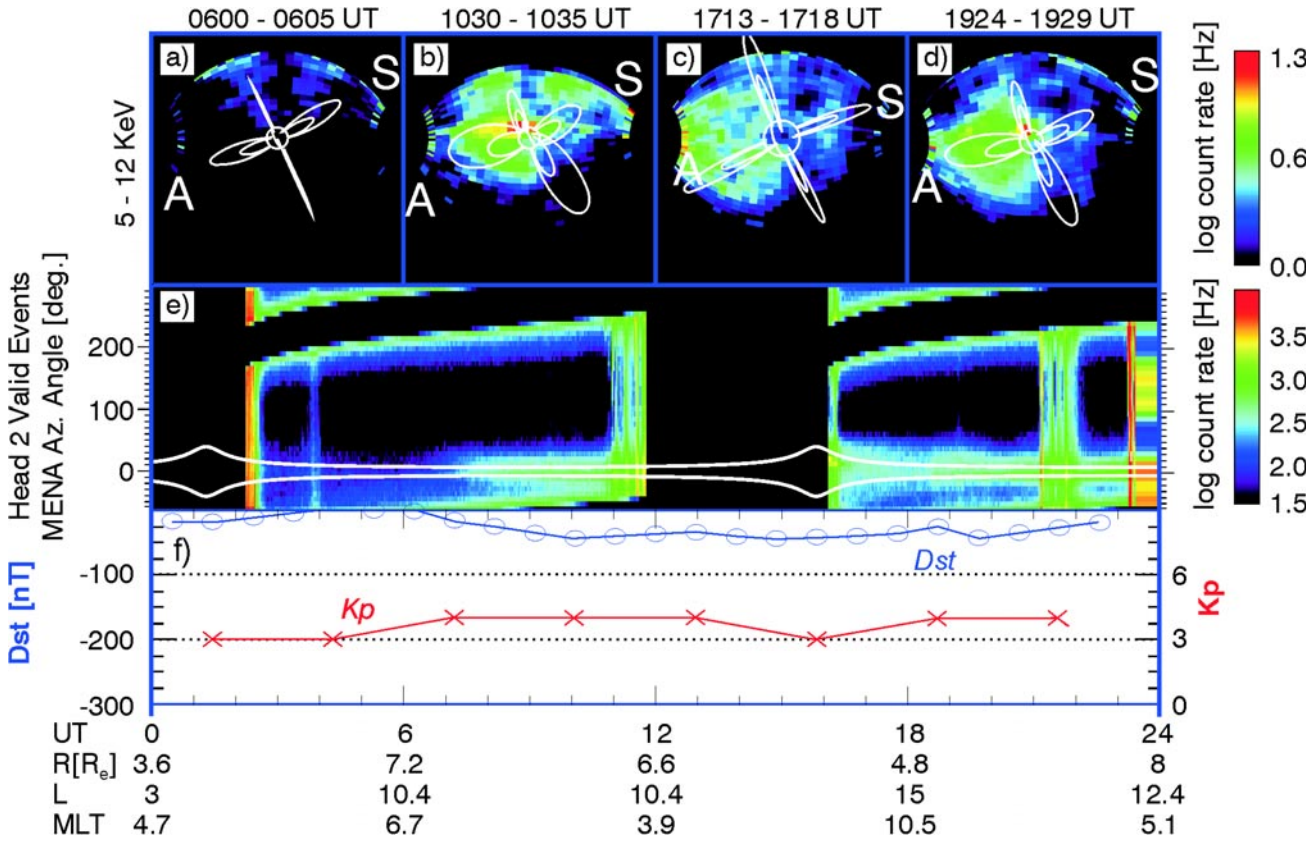

Figure 1. MENA observations and magnetospheric activity indices on July 26, 2000. Bottom panels show quantities plotted versus UT and orbital parameters. *Dst* (left) and *Kp* (right) appear in the bottom panel. The second panel from the bottom shows MENA coincidence rates, with IMAGE spin phase plotted on the ordinate and time on the abscissa. Two white lines indicate Earth's limb. Geophysical ENA emissions are ordered with respect to Earth. Detector voltages are reduced in the radiation belts, leaving gaps early on this day, and also between 1200–1600 UT. They are also reduced each spin for sunward viewing. Vertical bands of counts are due to charged particles energetic enough to overcome the electrostatic collimator deflection. The four panels across the top show 4-minute MENA images. Each is annotated with geomagnetic dipole field lines at MLT = 6, 12, 18, and 24 hours and at $L = 4$ and $L = 8$. Noon and midnight field lines are labeled "S" (sunward) and "A" (anti-sunward). The circle at the center of each image indicates Earth. The four images are of ENAs from 5.2–12 keV, assuming the species is hydrogen. Separate color bars to the right provide logarithmic scaling for the coincidence rates and the images.

Figure 1e shows few ENA counts through the first quarter of the day. Beginning near 0615 UT, counts are observed from near Earth. These are due to ENAs from the ion injection that gives rise to increases in *Kp* and *Dst*. After 1600 UT, ENA fluxes subside and broaden due to reduced activity and the lower IMAGE altitude. Then, near 1830 UT, another injection yields enhanced count rates of ENAs and a small increase in *Kp*.

ENA images from before and after the first ion injection are shown in a 180° fisheye projection in Figures 1a (0600–0604 UT) and 1b (1030–1034 UT). Few ENAs are observed prior to the onset of activity (1a, 1e). Subsequently (1b), substantial emissions from the anti-sunward region are seen, as expected for a night side plasma injection (counts near the top of the image are due to contamination from the sunward direction and should be ignored). Evident in these and other ENA images for specific observation geometries is the dominance of low altitude emissions. These originate from the MLT region opposite the spacecraft location and arise from the large density of charge exchange targets at low altitudes [*Roelof*, 1997]. As the magnetospheric activity subsides, so do the ENA fluxes, though not quite back to the low levels seen prior to 0615 UT.

Figures 1c (1715–1719 UT) and 1d (1910–1914 UT) show the inner magnetosphere before and after a second ion injection on July 26. Reduced fluxes are seen at 1715 UT, from an expanded volume as compared with those in 1b, still emanating primarily from the night side. Then, another injection is observed near 1830 UT (1d), on the night side.

August 12, 2000 Figure 2 displays observations of a geomagnetic storm on August 12, 2000, in a format similar to Figure 1. Images from three energy channels and at three times are arranged in columns (times) and rows (energy). We note here a saturation nechanism in MENA that is not yet fully understood. When the flux is large, we observe elongation in the imaging direction that is not geophysical. This is most evident in Figure 2g and 2h. It does not affect the main results of this paper, but will modify quantitative results in Table 1.

Dst peaked on this day near 1000 UT, at a value near −230 nT. ENA observations are obscured during the first seven hours of the day. There is a large difference between the MENA images obtained during the storm main phase and those obtained during late recovery. Emissions are more intense and localized at the earlier times (2a, 2d, and 2g)

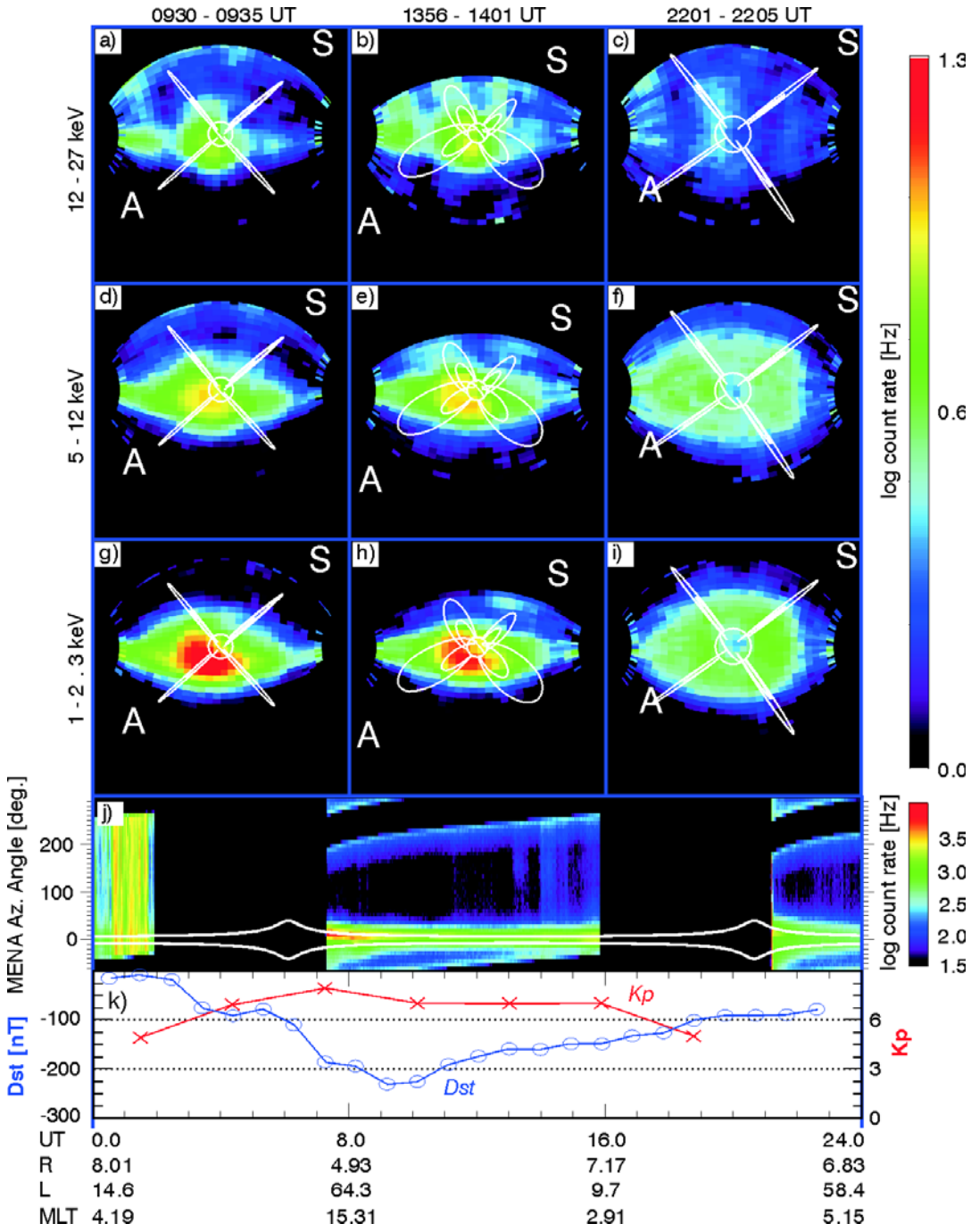

Figure 2. MENA observations and magnetospheric activity indices from August 12, 2000 (DOY 225). Format is similar to that of figure 1, except that 4-minute images in three energy ranges, assuming the species is hydrogen, are shown.

than they are later (2c, 2f, and 2i). The viewing geometry is similar and optimal (from over the pole) at the two times so that any effect due to viewing angle is minimal.

We can quantify ring current symmetry properties at these two times by measuring the ratio of counts in the dawn, noon, and dusk quadrants to those near midnight. Results for the energy range 5.2–12 keV are shown in Table 2. This demonstrates the asymmetry in the main phase ring current, as compared to the late recovery phase.

The center column (2b, 2g, 2h) shows the ring current during early recovery phase. The viewpoint here is from lower latitude. Viewing effects thus make it more difficult to determine the ring current distribution in MLT, nevertheless the emissions are clearly asymmetric.

These results are consistent across a range of MENA energies, though at the highest energy there are too few counts to confirm a symmetric ring current at 2240 UT. Most notably, the count rate decreases monotonically with energy.

Table 1. ENA counts from the dawn (0200–0900), noon (0900–1500), dusk (1500–2100), and midnight ("MN"; 2100–0300) MLT quadrants during storm main phase (0930 UT) and late recovery phase (2200 UT) are compared.

	$\frac{C^{dawn}}{C^{MN}}$	$\frac{C^{noon}}{C^{MN}}$	$\frac{C^{dusk}}{C^{MN}}$
0930 UT	0.63	0.45	0.77
2200 UT	0.99	0.98	1.2

This is driven both by the reduction of source ion flux and the decreasing charge exchange cross section with increasing ion energy.

3. Discussion

The near-Earth magnetosphere emits more ENAs during periods of geomagnetic activity than during quieter times [*Tinsley,* 1979]. MENA observations during mildly disturbed and storm times confirm this dependence. Further, they show a remarkable variety of emission morphology, owing to both geophysical and geometric viewing effects.

MENA imagery from the August 12, 2000, storm clearly shows evolution from asymmetric to symmetric ring current. The ratio of ENA flux from the noon quadrant to that from the midnight quadrant is ~ 0.45 during main phase and early recovery, and ~ 0.98 during the late recovery phase.

These observations confirm the existence of both partial and symmetric ring currents, a subject of current interest [*Grafe,* 1999; *Greenspan and Hamilton,* 2000]. Further, they show that the partial ring current evolves to a symmetric ring current at these energies over the life of the storm. Our observations suggest that the ring current lies mostly on open drift paths during storm main and early recovery phases and on closed drift paths during late recovery phase [*Liemohn et al.,* 1999].

Acknowledgments. We are grateful to many unnamed individuals at SwRI and collaborating institutions whose hard work has enabled these observations. We thank P. Gonzales and G. Waters for assistance in manuscript preparation. This work was supported at SwRI under NASA contract NAS5-96020.

References

Burch, J. L., Image Mission Overview *Sp. Sci. Rev.,* 91, 1, 2000.

essler A. J., and E. N. Parker, Hydromagnetic theory of geomagnetic storms, *J. Geophys. Res., 64*, 2239, 1959.

Fok, M.-C., et al., Ring current development during storm main phase, *J. Geophys. Res., 101,* 15311, 1996.

Frank, L. A., Direct detection of asymmetric increases of extraterrestrial 'ring current' proton intensities in the outer radiation zone, *J. Geophys. Res., 75,* 1263, 1970.

Grafe, A., Are our ideas about Dst correct?, *Ann. Geophys., 17,* 1, 1999.

Greenspan, M. E., and D. C. Hamilton, A test of the Dessler-Parker-Sckopke relation during magnetic storms, *J. Geophys. Res., 105,* 5419, 2000.

Henderson, M. et al., First energetic neutral atom images from Polar, *Geophys. Res. Lett., 24,* 1167, 1997.

Jorgensen, A., et al., Global energetic neutral atom (ENA) measurements and their association with the Dst index, *Geophys. Res. Lett., 24,* 24, 1997.

Kawasaki, K., and S.-I. Akasofu, Low-latitude DS component of geomagnetic storm field, *J. Geophys. Res., 76,* 2396, 1971.

Liemohn, M., et al., Analysis of early phase ring current recovery mechanisms during geomagnetic storms, *Geophys. Res. Lett., 26,* 2845, 1999.

Mitchell, D., et al., High Energy Neutral Atom (HENA) imager for the IMAGE mission, *Space Sci. Rev., 91*, 67-112, 2000. Moore, T. E., et al., The Low Energy Neutral Atom imager for IMAGE, *Space Sci. Rev., 91*, 155-195, 2000.

Pollock, C. J., et al., Medium Energy Neutral Atom (MENA) imager for the IMAGE mission, *Space Sci. Rev., 91,* 113, 2000.

Prölss, G. W., Decay of the magnetic storm ring current by the charge-exchange mechanism, *Planet. Space Sci., 21,* 983, 1973

Roelof, E. C., et al., Energetic neutral atoms from the ring current: IMP7/8 and ISEE1, *J. Geophys. Res., 90,* 10991, 1985.

Roelof, E. C., Energetic neutral atom image of a storm-time ring current, *Geophys. Res. Lett., 14,* 652, 1987.

Roelof, E. C., ENA emissions from nearly mirroring magnetospheric ions interacting with the exobase. *Adv. Space Res., 20,* 361, 1997.

Sckopke, N., A general relation between the energy of trapped particles and the disturbance field near the earth, *J. Geophys. Res., 71,* 3125, 1966.

Tinsley, B. A., Energetic neutral atom precipitation during magnetic storms—optical emission, ionization, and energy deposition at low and middle latitudes, *Geophys. Res. Lett., 6,* 291, 1979.

Williams, D. J., et al., Global magnetospheric imaging, *Rev. Geophys., 30,* 3, 183, 1992.

J. L. Burch, J.-M. Jahn, D. J. McComas C. J. Pollock and M. Wüest, SwRI, 6220 Culebra Road, San Antonio, TX 78238, USA. (e-mail: jburch@swri.edu; jjahn@swri.edu; dmccomas@swri.edu; cpollock@swri.edu; mwuest@swri.edu)

K. Asamura and T. Mukai, ISAS, 311 Yoshinodai Sagamihara, Kanagawa 229-8510, Japan

M. M. Balkey and E. Scime, WVU, Physics Department, Box 6315, Morgantown, WV 26506, USA.

H. O. Funsten, M. Henderson, S. Ritzau and R. Skoug, LANL, CSSE/NIS-1, Los Alamos, NM 87545, USA.

M. Grande, RAL, Oxfordshire OX11 0QX, England

M. Gruntman, USC, Department of Aerospace Engineering, Los Angeles, CA 90089-1191, USA.

M. Lampton, UCB, Space Sciences Laboratory, Centennial Drive at Grizzly Peak, Berkeley, CA 94720, USA.

M. W. Liemohn, UM, SPRL, 2455 Hayward St., Ann Arbor, MI 48109, USA.

M. L. Schattenburg, MIT CSR, 77 Mass. Ave., Cambridge, MA 02139, USA.

P. Valek, Auburn University, Department of Physics, 206 Allison Laboratory, Auburn, AL 36849, USA.

(Received November 13, 2000; revised January 15, 2001; accepted January 18, 2001.)